PTCR effect of solid solutions based on the (1-*x*)BaTiO$_3$–*x*Na$_{0.5}$Bi$_{0.5}$TiO$_3$ system

O.I. V'YUNOV[1]*, T.O. PLUTENKO[1], A.G. BELOUS[1], A.V. BILOUS'KO[1]

[1] *Department of Solid State Chemistry, Vernadskii Institute of General and Inorganic Chemistry,*
   32/34 Palladina Ave., 03142 Kyiv, Ukraine
* *Corresponding author. Tel./fax: +380-44-4242211; e-mail: vyunov@ionc.kiev.ua*

The structure and electrophysical properties of solid solutions based on the (1-*x*)BaTiO$_3$–*x*Na$_{0.5}$Bi$_{0.5}$TiO$_3$ ((1-*x*)BT–*x*NBT) system (0 ≤ *x* ≤ 0.6) were studied. Bulk samples were prepared by the solid-state reaction technique. Samples were sintered in air and in N$_2$ atmosphere with low concentration of H$_2$. The phase composition and the crystal structure were examined by X-ray powder diffraction for samples sintered in air. X-ray powder diffractometry (XRPD) analysis showed that in the (1-*x*)BaTiO$_3$–*x*Na$_{0.5}$Bi$_{0.5}$TiO$_3$ system *a* slightly increases, whereas *c* decreases with the substitution of Na and Bi ions for Ba ions. The permittivity was investigated in wide frequency and temperature ranges. Impedance analyses of samples sintered in N$_2$/H$_2$ atmosphere indicated that both the grain boundary and the outer layer region contribute to the positive temperature coefficient of resistivity (PTCR) effect in (1-*x*)BaTiO$_3$–*x*Na$_{0.5}$Bi$_{0.5}$TiO$_3$ ceramics.

Crystal structure / PTCR effect / Heterogeneous structure / Impedance analysis

1. Introduction

In recent years, a considerable interest has arisen in lead-free ceramics due to the restriction of the use of lead on the ground of human health and environmental protection [1]. The investigations of lead-free (1-*x*)BaTiO$_3$–*x*Na$_{0.5}$Bi$_{0.5}$TiO$_3$ ((1-*x*)BT–*x*NBT) ceramics with different electrical properties are of great scientific and practical interest. In particular, the dielectric properties [2-4] and the region of the morphotropic phase boundary [5] are investigated in this system. In the concentration range 1 ≤ *x* ≤ 0.88, the possibility of preparation of materials with a high level of piezoelectric properties is being examined [6-8].

In the (1-*x*)BaTiO$_3$–*x*Na$_{0.5}$Bi$_{0.5}$TiO$_3$ system at 0 < *x* ≤ 0.3, materials with positive temperature coefficient of resistivity (PTCR) effect can be prepared [9]. Without adding any additional donor dopant, a PTCR effect is found in pure (1-*x*)BT–*x*NBT ceramics at *x* ≤ 0.06 sintered in air [10]. It has also been shown that materials (*x* = 0.05) doped with niobium [9] and lanthanum [11] and sintered in air also exhibit the PTCR effect. At *x* > 0.06, PTCR ceramics can be prepared only in an atmosphere with low oxygen pressure. Ceramics with *x* ≈ 0.3 show PTCR properties comparable to those of lead-containing PTCR materials [12,13]. The PTCR effect can be increased by subsequent reoxidation in air at

800-1100°C [14], or by adding small amounts of manganese [15].

Previous studies have shown that the PTCR effect in materials based on barium titanate depends on the electrically heterogeneous grain structure [16]. Such materials consist of semiconducting grains, an outer layer with higher resistance and high-resistance grain boundaries. Literature data concerning the contribution of electrically heterogeneous grain structure to the PTCR effect are limited [12,15].

The aim of this work was therefore to study the PTCR effect in (1-*x*)BaTiO$_3$–*x*Na$_{0.5}$Bi$_{0.5}$TiO$_3$ (0 ≤ *x* < 0.6) solid solutions.

2. Experimental procedure

(1-*x*)BaTiO$_3$–*x*Na$_{0.5}$Bi$_{0.5}$TiO$_3$ solid solutions (where *x* = 0.04-0.3) were prepared by the solid-state reaction technique. Extra-pure (purity 99.99%) Na$_2$CO$_3$, BaCO$_3$, Bi$_2$O$_3$ and TiO$_2$ (rutile) were used as initial reagents for the preparation. The powders were mixed and ball-milled with ethyl alcohol in an agate mortar for 4 h. After evaporating the residual water, the mixtures were dried at 100-120°C, passed through a capron sieve, and then calcined in air at 950-1000°C for 2-4 h. The resultant powders were ground with the addition of 10% polyvinyl alcohol, pressed into pellets (10 mm in diameter and 2 mm in thickness) by uniaxial pressing at 150 MPa.

Table 1 Structure parameters of samples in the $(1-x)BaTiO_3-xNa_{0.5}Bi_{0.5}TiO_3$ system. Space group *P4mm* (99), the positions of the ions are the following: Ba/Na/Bi (1*b*) 1/2 1/2 *z/c*, Ti (1*a*) 0 0 0, O1 (1*a*) 0 0 *z/c*, O2 (2*c*) 1/2 0 *z/c*.

x	0.00	0.08	0.09	0.10	0.20	0.60
Unit cell parameters						
a, Å	3.9941(2)	3.9976(2)	3.9980(2)	3.9981(2)	3.9983(2)	3.9986(2)
c, Å	4.0337(2)	4.0303(2)	4.0285(3)	4.0280(3)	4.0271(3)	4.0211(3)
c/a	1.010	1.008	1.008	1.007	1.007	1.006
V, Å^3	64.349(5)	64.407(5)	64.391(7)	64.387(7)	64.378(6)	64.292(7)
Atom coordinates						
Ba/Na/Bi: z/c	0.49(1)	0.49(1)	0.49(2)	0.48(2)	0.482(8)	0.49(1)
O1: z/c	0.51(2)	0.54(2)	0.53(3)	0.52(3)	0.51(2)	0.50(6)
O2: z/c	0.02(2)	0.04(5)	0.01(3)	0.01(3)	0.03(3)	0.02(5)
Agreement factors						
R_B, %	4.04	5.54	6.82	5.62	5.48	9.81
R_f, %	2.78	4.22	4.81	3.71	3.51	8.54
R_{exp}, %	5.83	7.47	7.98	7.68	7.31	8.59

For dielectric measurements, the pellets were sintered in air in the temperature range 1200-1330ºC with subsequent deposition of silver electrodes on the polished surfaces of the samples. To study the PTCR effect pellets were synthesized in a flow of a gas mixture N_2/H_2 (97:3) at 1310ºC with subsequent deposition of aluminum electrodes on the polished surfaces of the samples. The heating and cooling rates for all samples were 300°C/h.

The phases were characterized by X-ray powder diffractometry (XRPD) a using DRON-4-07 diffractometer (Cu Kα radiation; 40 kV, 20 mA). The structure parameters were refined by the Rietveld full-profile analysis. XRPD patterns were collected in the range 2θ = 10-150° in step-scan mode with a step size of $\Delta2\theta$ = 0.02° and a counting time of 10 s per data point. As external standards, we used SiO_2 (for 2θ) and Al_2O_3 NIST SRM1976 (for the intensity).

The temperature dependence of the electrical resistance of the samples was measured in the temperature range 20°C to 400°C. Impedance data were obtained using a 1260 Impedance / Gain-phase Analyzer (Solartron Analytical) in the range 100 Hz to 1 MHz. The components of the equivalent circuit were identified using ZView software (Scribner Associates).

3. Results and discussion

The XRPD patterns of the powders fired at temperatures lower than 1000°C contain reflections of several phases. The $BaTiO_3$-based phase was the dominant one within the entire temperature range. For samples with $x \geq 0.3$, trace amounts of the $Ba_6Ti_{17}O_{40}$ phase were also observed. After heat treatments above 1050°C, all the examined samples were single-phase ones. The parameters of the crystal structure of the ceramic samples were determined by means of Rietveld full-profile X-ray analysis (Fig. 1).

As shown in Table 1 the substitution of Na and Bi for Ba affects the unit cell parameters of the samples in the $(1-x)BaTiO_3-xNa_{0.5}Bi_{0.5}TiO_3$ system. The parameter a slightly increases, whereas c decreases with the substitution of Na and Bi ions for Ba ions. The dependence of the unit cell volume on the concentration of sodium and bismuth passes through a maximum at x = 0.08. The subsequent decrease in the unit cell volume with increasing x is due to the smaller ionic radii of Na and Bi (1.18 Å and 1.17 Å respectively) in comparison with Ba (1.42 Å) [17].

Fig. 2(a) shows the dielectric permittivity as a function of temperature for the sintered ceramics of $(1-x)BaTiO_3-xNa_{0.5}Bi_{0.5}TiO_3$ solid solutions at 100 kHz. As x increases the temperature of maximum $\varepsilon(T)$, which corresponds to a phase transition temperature, increases (inset in Fig. 2(a)). Above the Curie point the dielectric permittivity of the studied compositions obeys the Curie-Weiss law. In this case, the magnitude of the Curie-Weiss constant monotonously increases from $1.7 \cdot 10^5$ K (x = 0) to $1.2 \cdot 10^6$ K (x = 0.6).

It should be noted that in $(1-x)BaTiO_3-xNa_{0.5}Bi_{0.5}TiO_3$-based materials with higher x ($0.88 \leq x \leq 1$) two peaks were observed on plots of $\varepsilon(T)$ [7]. This may be accounted for by the fact that in materials with high x, the polarization mechanism is similar to that in $Na_{0.5}Bi_{0.5}TiO_3$. The $Na_{0.5}Bi_{0.5}TiO_3$-based phase has two peaks (at T_1 = 175 C and T_2 = 320°C) on the plot of $\varepsilon(T)$ [7]. In materials with lower x ($0 \leq x \leq 0.6$) the polarization mechanism is similar to that in $BaTiO_3$, in which there is one peak (at T = 120°C) on the plot of $\varepsilon(T)$ [18].

Fig. 2(b) shows the temperature dependence of the resistivity in $(1-x)BaTiO_3-xNa_{0.5}Bi_{0.5}TiO_3$ solid solutions, for samples with x = 0.08, 0.1 and 0.3. The PTCR effect is observed at temperatures above the phase transition temperature.

The plot of ρ_{min} against concentration shows a minimum at x = 0.1 (inset in Fig. 2(b)). Similar
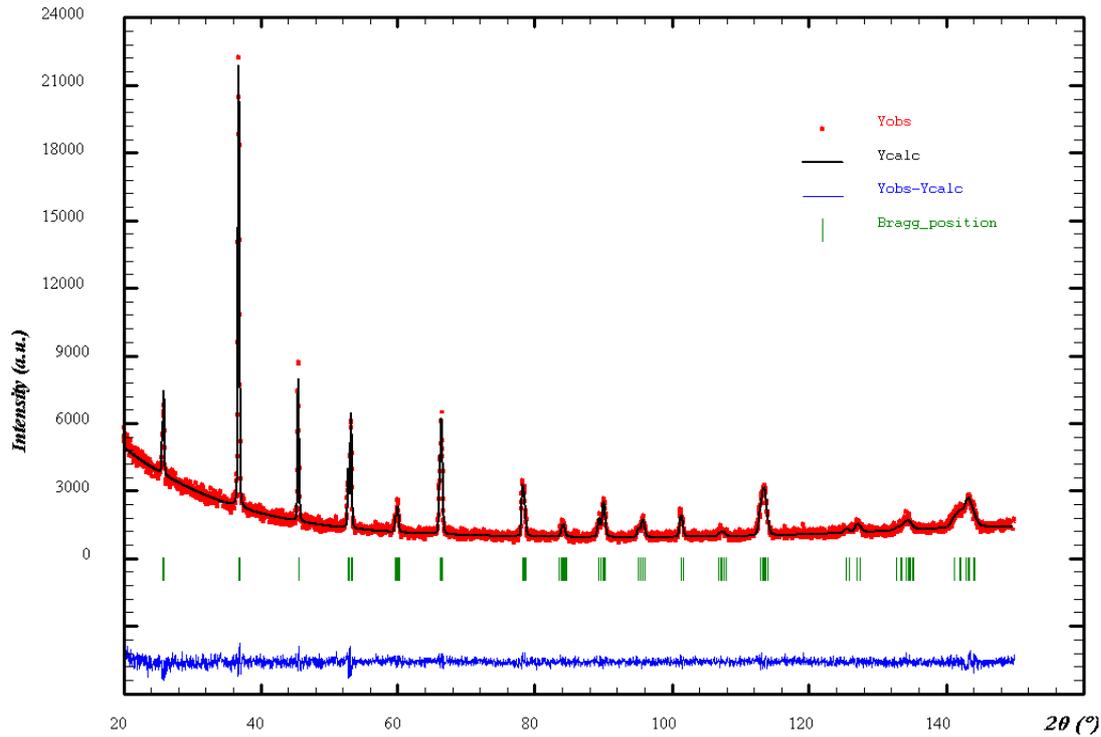
Fig. 1 Experimental (dots) and calculated (line) room-temperature powder X-ray diffraction patterns of (1-*x*)BaTiO$_3$–*x*Na$_{0.5}$Bi$_{0.5}$TiO$_3$ ceramics: *x* = 0.09. Bars indicate the peak positions.
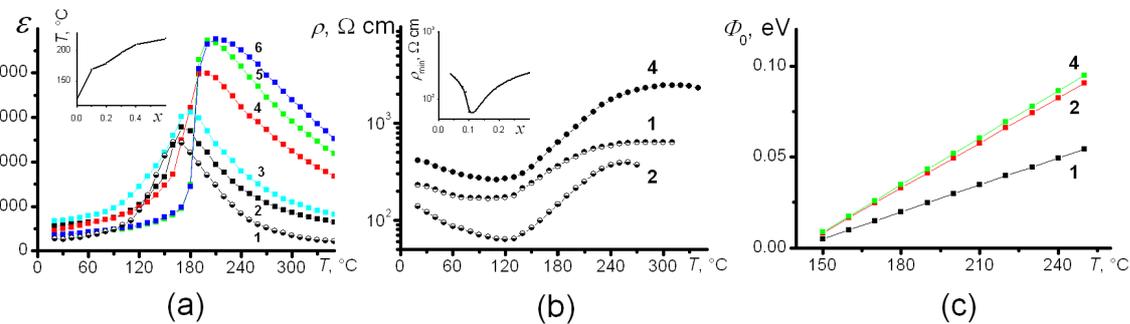
Fig. 2 Temperature dependence of the dielectric permittivity (a), resistivity (b) and intergranular barrier height (c) of (1-*x*)BaTiO$_3$–*x*Na$_{0.5}$Bi$_{0.5}$TiO$_3$ ceramics, *x* = 0.08 (1); 0.1 (2); 0.2 (3); 0.3 (4); 0.4 (5); 0.6 (6); *f* = 100 kHz. Insets: Variation of the Curie temperature (a) and minimum values of resistivity (b) for (1-*x*)BaTiO$_3$–*x*Na$_{0.5}$Bi$_{0.5}$TiO$_3$ ceramics as a function of *x*.

dependence was observed in [15]. This dependence could be explained by two processes: increase of the amount of conducting electrons in grains at low concentration and increase of the number of acceptor states at the grain boundary at high concentration. For low *x* (0 ≤ *x* ≤ 0.1), segregation of Na$^+$ ions occurs at the grain boundaries, which causes an excess of Bi^{3+} ions in the grain bulk. In the position of barium, the Bi^{3+} ion has an excess positive charge. This excess positive charge is compensated by electrons, which leads to the appearance of semiconducting properties and decrease of resistivity. For higher *x* (0.1 ≤ *x* ≤ 0.3), excess positive charge is compensated

by cation vacancies, and hence the resistivity increases [15].

The temperature dependence of the resistivity in PTCR ceramics consists of three distinct portions [16]. In regions I and III, the variation of the resistivity with temperature is similar to that in semiconductors and dielectrics, respectively. In region II, the resistance rises rapidly with increasing temperature. In the PTCR effect, changes in resistivity can be described using the Heywang model [19]. In accordance with this model there are surface acceptor states that lead to the formation of potential barriers at the grain boundaries. The height of the intergranular barriers of the

$(1-x)BaTiO_3–xNa_{0.5}Bi_{0.5}TiO_3$ system was calculated. In region I, the variation of resistance with temperature is described by the equation [19,20]:

$$\rho_S = \rho_0 \cdot e^{\frac{E_a^I}{kT}} \tag{1}$$

where ρ_0 is a constant, E_a^I is the activation energy for conduction in region I, and k is the Boltzmann constant. A similar equation is applicable to region III [19,20]:

$$\rho_d = \rho_0^d \cdot e^{\frac{E_a^{III}}{kT}} \tag{2}$$

where E_a^{III} is the activation energy for conduction in region III.

The variation of resistance with temperature in region II (PTCR behavior) is described by the equation [19]:

$$\rho = \alpha \cdot \rho_S \cdot e^{\frac{\Phi_0(T)}{kT}} \tag{3}$$

where α is a geometric factor, and $\Phi_0(T)$ is the intergranular barrier height:

$$\Phi_0(T) = \frac{e^2 \cdot n_D \cdot b^2}{2 \cdot \varepsilon_i(T) \cdot \varepsilon_0} \tag{4}$$

Here, e is the electronic charge ($1.602 \cdot 10^{-19}$ C), n_D is the bulk electron concentration, b is the barrier thickness ($2 \cdot b = \frac{n_S}{n_D}$, where n_S is the surface concentration of acceptor states), and $\varepsilon_i(T)$ is the permittivity of the grain bulk. In ferroelectrics, ε_i obeys the Curie-Weiss law: $\varepsilon_i(T) = \frac{C}{T - \Theta}$, where C is the Curie constant, and Θ is the Curie temperature (for example, in barium titanate, $C = 1.7 \cdot 10^5$ K; $\Theta = 383$ K [20])

From Eqs. (1) and (3), we obtain:

$$\rho = \alpha \cdot \rho_0 \cdot e^{\frac{E_a^I}{kT}} \cdot e^{\frac{e^2 \cdot n_D \cdot b^2 (T-\Theta)}{2 \cdot \varepsilon_0 \cdot C \cdot kT}} \tag{5}$$

The results of the calculations in accordance with equations (1) and (5) indicate that with increasing x in region I the value of ρ_0 passes through a minimum, and the activation energy passes through a maximum ($\rho_0 = 27.9$, 5.4 and 38.5 Ω cm and $E_a^I = 0.05$, 0.08 and 0.06 eV for $x = 0.1$, 0.08 and 0.3, respectively).

The results thus obtained were used to calculate, using Eq. (4), the intergranular barrier height Φ_0 as a function of x in region II, where the resistance rises drastically. It can be seen that with increasing x, the intergranular barrier grows (Fig. 2(c)), which can be attributed to an increase in the number of acceptor states at the grain boundaries, for example, due to the segregation of Na$^+$ ions [15].

The results of the frequency investigation of PTCR ceramics $(1-x)BaTiO_3–xNa_{0.5}Bi_{0.5}TiO_3$ can be analyzed as four types of dependences: complex impedance (Z^*), complex admittance (Y^*), complex permittivity (ε^*), and complex electric modulus (M^*) [21-23]. These complex quantities are interrelated:

$M^* = 1/\varepsilon^* = j\omega CoZ^* = j\omega Co(1/Y^*)$, where ω is the angular frequency and Co is the capacitance of empty cell (where $j = \sqrt{-1}$). Initially, the results of the frequency investigation of PTCR materials were obtained as $Z'' = f(Z')$ relations (Fig. 3). This plot is convenient for the determination of the components of the equivalent circuit. For further analysis, the results of the investigation of the complex impedance were also represented as frequency dependencies of the imaginary components of the complex impedance Z'' and complex electric modulus M'' (Fig. 4). In the case of parallel RC elements, the frequency dependencies of Z'' and M'' are described by the equations [22-24]:

$$Z'' = R \frac{\omega RC}{1 + (\omega RC)^2} \tag{6}$$

$$M'' = \frac{\varepsilon_0}{C} \cdot \frac{\omega RC}{1 + (\omega RC)^2} \tag{7}$$

where $\omega = 2\pi f$ ($f =$ frequency in Hz), and ε_0 is the permittivity ($8.854 \cdot 10^{-14}$ F cm^{-1}).
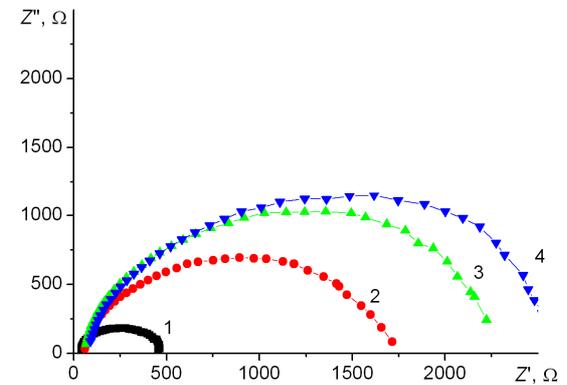
Fig. 3 Complex impedance diagram of $(1-x)BaTiO_3–xNa_{0.5}Bi_{0.5}TiO_3$ ($x = 0.09$) ceramics at 144°C (1), 204°C (2), 267°C (3) and 314°C (4).
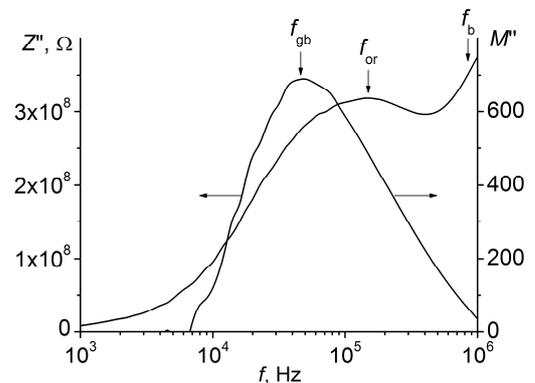
Fig. 4 Imaginary parts of the combined impedance (Z'') and modulus (M'') for $(1-x)BaTiO_3–xNa_{0.5}Bi_{0.5}TiO_3$ ($x = 0.09$) ceramics; the grain outer layer is marked as "or", the grain boundary as "gb", and the grain bulk as "b".
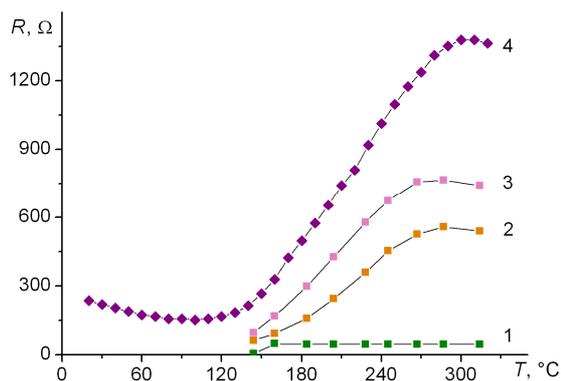
Fig. 5 Resistance of the grain bulk (1), outer layer (2), grain boundary (3) and overall resistance (4) of (1-*x*)BaTiO₃-*x*Na₀.₅Bi₀.₅TiO₃ (*x* = 0.09) ceramics.

From Eqs. (6) and (7) it follows that:

$$\omega_{max} = \frac{1}{RC} \qquad (8)$$

$$Z''_{max} = \frac{R}{2} \qquad (9)$$

$$M''_{max} = \frac{\varepsilon_0}{2C} \qquad (10)$$

Equations (8)-(9) show that the shift in the positions of Z''_{max} and M''_{max} on the frequency axis is associated with a change in the values of both the capacity and the resistance in the corresponding RC element.

Fig. 4 shows that the peaks Z''_{max} and M''_{max} do not coincide in frequency. This indicates that the positions of the above maximums are determined by different areas of the ceramics. We interpreted the experimental results by using the model of PTCR for ceramic grains proposed by Sinclair and West [24]. According to this model, the inner fraction of a grain has semiconducting properties, whereas the grain boundaries have dielectric properties. Between these two areas there exists a transition region, in which the resistivity is higher than in the semiconducting inner region, but lower than in the grain boundary dielectric layer. These areas of ceramics are electrically non-uniform and can be represented by an equivalent circuit, which includes three parallel RC elements connected in series. In particular, the change in the value and positions of the maximums of $Z''(f)$ and $M''(f)$ are determined by the electrophysical properties of the following grain fractions: the grain boundaries determine the plot of $Z''(f)$, the grain outer layer is responsible for the plot of $M''(f)$ in the middle of the measuring frequency range, whereas the grain bulk determines the plot of $M''(f)$ at frequencies over 10^8 Hz. These areas can also be distinguished using the plot $Z'' = f(Z')$ (see Fig. 3).

The results of the analysis show that it is possible to distinguish the properties of the grain bulk, grain boundary and the outer layer only above 140°C

(Fig. 5). As is seen from Fig. 5, the resistance of the grain bulk varies little in the investigated temperature range (Fig. 5, curve 1). At the same time, the temperature dependencies of the resistance of the grain boundary and the outer layer pass through a maximum (Fig. 5, curves 2 and 3). This indicates that both the grain boundary and the outer layer region contribute to the PTCR effect in the studied materials.

Conclusions

The results of the investigations show that in the (1-*x*)BaTiO₃–*x*Na₀.₅Bi₀.₅TiO₃ (0 ≤ *x* <0.6) system, only one maximum exists on the plot of the dielectric permittivity against temperature $\varepsilon(T)$. This may be accounted for by the fact that the polarization mechanism in this system is similar to that in BaTiO₃.

The change in resistivity for the PTCR effect of the (1-*x*)BaTiO₃–*x*Na₀.₅Bi₀.₅TiO₃ (0 ≤ *x* <0.3) system can be described using the Heywang model. Calculations of the intergranular barrier height Φ_0 showed that the magnitude of the potential barrier increases with increasing *x*.

The grain boundary and the outer layer region contribute to the PTCR effect in the (1-*x*)BaTiO₃–*x*Na₀.₅Bi₀.₅TiO₃ (0 ≤ *x* <0.3) system.

References

[1] Directive 2002/95/EC of the European Parliament and of the Council of 27 January 2003 on the restriction of the use of certain hazardous substances in electrical and electronic equipment, *Off. J. Eur. Union* 37 (2003) 19-23.
[2] Lanfang Gao, *Ceram. Int.* 33 (2007) 1041-1046.
[3] Yanfang Qu, *Mater. Sci. & Eng. B* 121 (2005) 148-151.
[4] Bok-Hee Kim, *Ceram. Int.* 33 (2007) 447-452.
[5] P. Jarupoom, *Current Appl. Phys.* 8 (2008) 253-257.
[6] H.Y. Tian, *Solid State Commun.* 142 (2007) 10-14.
[7] Min Chen, *J. Eur. Ceram. Soc.* 28 (2008) 843-849.
[8] Dunmin Lin, *Solid State Ionics* 178 (2008) 1930-1937.
[9] H. Takeda, T. Shimada, *J. Electroceram.* 22 (2009) 263-269.
[10] P.-H. Xiang, H. Takeda, T. Shiosaki, *Jpn. J. Appl. Phys.* 46 (2007) 6995.
[11] H. Takeda, W. Aoto, T. Shiosaki, *Appl. Phys. Lett.* 87 (2005) 102104.
[12] P.-H. Xiang, H. Takeda, T. Shiosaki, *Appl. Phys. Lett.* 91 (2007) 162904.
[13] T. Shimada, K. Touji, *J. Eur. Ceram. Soc.* 27 (2007) 3877-3882.

[14] Wei Jifeng, Pu Yongping, Mao Yuqin, Wang Jinfei, *J. Am. Ceram. Soc.* 93(6) (2010) 1527-1529.

[15] P.-H. Xiang, H. Takeda, T. Shiosaki, *J. Appl. Phys.* 103 (2008) 064102.

[16] O.I. V'yunov, L.L. Kovalenko, A.G. Belous, V.N. Belyakov, *Inorg. Mater.* 39(2) 2003 190-197.

[17] R.D. Shannon, *Acta Crystallogr. A* 32 (1976) 751.

[18] P. Duran, D. Gutierrez, *Ceram. Int.* 28 (2002) 283-292.

[19] W. Heywang, *J. Am. Ceram. Soc.* 47(10) (1964) 484-490.

[20] W. Heywang, *J. Mater. Sci.* 6 (1971) 1214-1226.

[21] D.C. Sinclair, F.D. Morrison, A.R. West, *Int. Ceram.* 2 (2000) 33-37.

[22] F.D. Morrison, D.C. Sinclair, A.R. West, *J. Am. Ceram. Soc.* 84(2) (2001) 474-476.

[23] F.D. Morrison, D.C. Sinclair, A.R. West, *J. Am. Ceram. Soc.* 84(3) (2001) 531-538.

[24] D.C. Sinclair, A.R. West, *J. Am. Ceram. Soc.* 78(1) (1995) 241-244.

_____